International Journal of Geo-Information

MDPI

Article

Assessing the Distribution of Urban Green Spaces and its Anisotropic Cooling Distance on Urban Heat Island Pattern in Baotou, China

Tongliga Bao [1,2], Xueming Li [1,3,*], Jing Zhang [4,†], Yingjia Zhang [1] and Shenzhen Tian [1]

1 College of Urban and Environmental Sciences, Liaoning Normal University, Dalian 116029, China; tongliga113@126.com (T.B.); zyj575657@163.com (Y.Z.); shenzhen890038@163.com (S.T.)
2 College of Resources and Environment, Baotou Teachers' College, Baotou 014030, China
3 Institute of Human Settlement, Liaoning Normal University, Dalian 116029, China
4 College of Environment and Resources, Dalian Nationalities University, Dalian 116600, China; zhangjing@dlnu.edu.cn
* Correspondence: lixueming999@163.com; Tel.: +86-411-8215-8258
† These authors contributed equally to this work.

Academic Editor: Wolfgang Kainz
Received: 29 December 2015; Accepted: 28 January 2016; Published: 6 February 2016

Abstract: An essential part of urban natural systems, urban green spaces play a crucial role in mitigating the urban heat island effect (UHI). The UHI effect refers to the phenomenon where the temperature within a city is higher than that of the surrounding rural areas. The effects of the spatial composition and configuration of urban green spaces on urban land surface temperature (LST) have recently been documented. However, few studies have examined the effects of the directionality and distribution of green spaces on LST. In this study, we used a landscape index to describe the change in pattern of heat island intensity for the city of Baotou, China. We then used a semi-variable function and nearest neighbor algorithm to analyze the cooling effects of green spaces. We found that: (1) the cooling distance of an urban green space was not only influenced by its size, vegetation cover, and shape, but also showed anisotropy. In general, the larger the area of the urban green space and the higher the value of Normalized Difference Vegetation Index (NDVI; a measure of plant photosynthetic activity), the larger the cooling distance within a certain threshold. Green spaces with more regular shapes displayed higher LST mitigation; however, the cooling distance was directional, and cooling effects depended on the semi-major axis and semi-minor axis of the green space. (2) The distribution of the urban green space within the landscape played a key role in mitigating the UHI effect. Within a certain area, the cooling effect of green spaces that are evenly distributed was greater than that which was associated with either green spaces that were large in area or where greens spaces were aggregated in the landscape. Therefore, within urban areas, where space is limited, urban planning should account for green spaces that are relatively scattered and evenly distributed to maximize cooling effects. The results of this study have key implications for sustainable urban planning and development; to mitigate urban heat island effects it is important to not only increase canopy cover or the size of urban green spaces, but also to optimize their spatial configuration.

Keywords: urban green space; cooling effects; urban heat island pattern; Baotou City

1. Introduction

Urban areas are becoming increasingly important and the United Nations projects that more than 65% of the global population will be urban dwellers by the year 2050 [1]. It is therefore essential to work towards a better understanding of the complex processes that are involved with

sustainable development and human well-being in cities. The urban heat island (UHI) effect refers to the phenomenon where the temperature within a city is higher than that of the surrounding rural areas [2–4]. The reduced natural surroundings, high exhaust heat emissions, increased impervious surface and surface roughness, and narrow urban skyline associated with cities often results in this increased temperature effect [5,6]. The UHI not only alters the urban thermal environment, but also increases the likelihood of extreme heat events, enhances air pollution, increases energy consumption, and threatens human health [7–9]. Thus, more research into the UHI effect and how to mitigate it [10,11] will be of great importance for effective improvement of the urban ecological environment and to improve the conditions of human settlements within cities [12].

Providing key ecological functions and services (e.g., carbon storage, soil conservation, noise buffering, air quality, *etc.*) within areas of urban expansion, urban green spaces are an essential part of the urban ecosystem. In addition, they also provide a cooling role through evaporation and shading effects which help to mitigate UHI effects [13–15]. Different factors which contribute to the cooling effects provided by urban green spaces have been reported in the literature, such as plant-specific properties, single park cooling effects of urban vegetation, and the cooling effect of green spaces on their surrounding areas [16]. For example, trees with needle leaves have a lower leaf density than broad leaved trees, allowing more solar radiation to penetrate to the ground surface increasing the land surface temperature (LST), thus providing a lower cooling function than that of broad leaves [17]. A comparison between vegetation types identified that the cooling effect of urban green space vegetation declines from arbor, having the largest cooling effect, through shrub to herbage, having the lowest cooling effect [18]. The more internal water bodies located within an urban green space, the lower the internal temperature of that space, which usually provides a significant cooling effect [19,20]. It has also been shown that surface temperature differences within a city are correlated with the amount of vegetation, with areas with more vegetation associated with cooler surface temperatures [21,22]. The amount of vegetation coverage and normalized difference vegetation index (NDVI; a measure of plant photosynthetic activity) are negatively correlated to UHI [23–25].

The relationship between the intensity of the UHI effect and the spatial pattern of green spaces, as well as their composition and configuration has also been documented recently. Green space composition refers to the abundance and variety of land cover types (*i.e.*, size, density, and evenness of urban green space patches), and configuration is related to the spatial arrangement and layout (*i.e.*, shape, aggregation, and cohesion of patches) [26,27]. Numerous studies have shown that the size of urban green space is a better indicator of its cooling effect [11,28]. It was found that green spaces of average-size (~0.5×10^6 m^2) usually have a temperature reduction range of 1.5–3.0 °C [13,29,30], while larger green spaces (>1.5×10^6 m^2) have a more substantial cooling effect on their surrounding environment [31]. Based on a case study of Beijing, a highly urbanized metropolitan area in China, an increase of 10% in percent cover of green space would result in a 0.86 °C decrease in LST [32]. In addition, the configuration of green spaces also affects the cooling efficiency. Holding composition constant, Zhou *et al.* (2011) suggested that UHI can be mitigated by optimizing urban land cover spatial configuration [27]. In another study, green spaces that were simple in shape were shown to have a more substantial cooling effect than those that were complex in shape [11]. Although, many studies have examined the effects of configuration of green spaces on UHI intensity [32,33], configuration factors, such as the anisotropic influence of the cooling distance and distribution of urban green spaces on heat islands were rarely examined. These factors might provide insights for optimizing the configuration of green spaces to mitigate UHI effect via urban planning. For this reason, our objectives were: (1) to use a semi-variance function to examine the cooling distance (the geographic distance of the cooling effect) of urban green spaces to examine whether differences exist between different directions of urban green spaces in terms of cooling distance, and to determine whether differences were related to the shape and size of green spaces; and (2) to discover whether the spatial distribution of urban green spaces would change the heat island pattern, and, if so, which type of distribution (aggregation or scattering) had the strongest effect on the UHI.

2. Materials and Methods

2.1. Study Area

Baotou, the largest city of the Inner Mongolia Autonomous Region and an important industrial center of China, is located within western Inner Mongolia between 109°25′E and 110°25′E longitude and 40°25′N and 40°50′N latitude (Figure 1). The administrative area of Baotou covers 11 districts and a total area of 2.776×10^{10} m^2, and has a metropolitan area covering 2.2×10^8 m^2, a population of 2,799,200 and includes four districts; Kundulun, Qingshan, Donghe, and Jiuyuan. Baotou has a temperate continental climate with a mean annual temperature of 6.4 °C, an average total annual rainfall of 310 mm, and a total of 110–143 frost-free days.

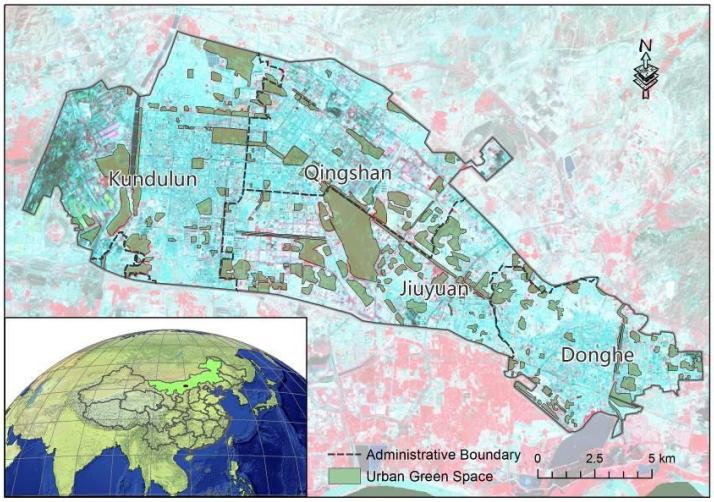

Figure 1. Location map of the study area.

2.2. Data and Processing

We used 30 m resolution remote sensing images from Landsat 5 TM taken in 2000, 2004, 2007, and 2011, and Landsat 8 OLI from 2014. We downloaded these images, which were captured during the growing season (July through August), from the US Geological Survey website. Images were only selected if they had cloud cover of 2% or below. We conducted radiometric calibration, atmospheric correction, geometric correction (single-point precision below 1 pixel), masking and other treatments on image data from all five time periods using ENVI5.1 and ArcGIS10.3. We then extracted urban green spaces found within Baotou by screen visual interpretation. We conducted an accuracy assessment of our urban green space classification using ground truthing from an independent field study, and our classification accuracy was 95% or higher.

2.3. Research Methods

2.3.1. Land Surface Temperature (LST)

We adopted the mono-window algorithm to retrieve the LST with a spatial resolution of 30 m from Landsat TM/OLI TIR channel [34]. The formulas are as follows:

$$T_s = [a_6 (1 - C_6 - D_6) + [b_6 (1 - C_6 - D_6) + C_6 + D_6] T_6 - D_6 T_a] / C_6 \quad (1)$$

$$T_6 = K_2 / ln (1 + K_1 / L_\lambda) \quad (2)$$

$$C_6 = \varepsilon_6 \tau_6 \quad (3)$$

$$D_6 = (1 - \varepsilon_6) [1 + (1 - \varepsilon_6) \tau_6] \quad (4)$$

where, T_s is the real ground temperature (K); T_6 is brightness temperature (K); L_λ is radiance (mW/(cm^2· sr· μm)), K_1 and K_2 are constants (mW/(cm^2· sr· μm) and K) obtained from the Landsat image header; ε_6, τ_6, and T_a are surface emissivity, atmospheric transmittance and average atmospheric temperature (K), respectively. The surfaces were mainly divided into three types, *i.e.*, water, urban, and natural surfaces. The ε_6 of water was taken as 0.995 and the urban and natural surface were estimated from vegetation coverage. The τ_6 was calculated using the LOWTRAN7 atmospheric model, and T_a was calculated using the standard atmosphere section average temperature [34]: $a_6 = -67.355$, $b_6 = 0.458$ (temperature range of 0–70 °C).

2.3.2. Spatial Pattern of UHI Intensity

To account for variability in the temperature obtained from remote sensing images over several time periods, we used the following Equation (5) to calculate the relative temperature (°C) and then divided the UHIs intensity into different grades using this threshold value (Table 1):

$$R = (T_{ui} - T)/T \quad (5)$$

where, T_{ui} is brightness of the ith study area, and T is the average ground temperature of Baotou.

Table 1. Grading standard of UHIs.

R	UHI Grade	Meaning
<−0.1	1	None
−0.1 to −0.05	2	Weak
−0.05 to 0.00	3	Moderate
0.00 to 0.05	4	Strong
0.05 to 0.15	5	Very strong
>0.15	6	Extremely strong

Landscape metrics were also selected to describe the pattern of UHI intensity within each grade, such as Class Area (CA), Number of Patches (NP), Landscape Shape Index (LSI), Aggregation Index (AI), Shannon's Evenness Index (SHEI), Mean Patch Fractal Dimension (FRAC_MN), and Perimeter-Area Ratio (PARA). These indices were all calculated using the software Fragstats 4.2. The CA is equal to the sum of the area of all patches with the corresponding patch type (m^2) and the NP refers to the number of patches of the same patch type. The LSI provides a standardized measure of total edge or edge density of a patch while adjusting for the size of the overall landscape, and, when LSI > 1, the higher the value the larger the degree of landscape fragmentation. The AI is a measure of the relative degree of aggregation of patches in the landscape, ranging from 0 to 100 %, in which a greater value represents a higher degree of patches that are clumped. The SHEI considers an even distribution of area among patch types to be a landscape with maximum evenness; when the value is 0, it means that there is only one kind of patch and when the value is 1, it suggests the uniform distribution of different patch types. The FRAC_MN ranges from 1 to 2, and provides a measure of patch size and the degree of convolution of its border, in which the greater the value, the more complex the shape. The PARA is a simple measure of shape complexity, in which the greater the value, the more complex the shape.

SPSS 20.0 statistical software was used to analyze the relationship between the isotropic cooling distance and urban green space area, and between the mean NDVI, with a spatial resolution of 30 m, and the shape index of green spaces (PARA).

Six typical sampling areas were also selected in urban green spaces which were defined as aggregates. We generated ten equal interval (30 m interval) buffers, from 0 m–300 m around the urban green space aggregates, and we calculated the mean surface temperature of each for the five time periods of Landsat images.

2.3.3. Cooling Distance and Direction of Urban Green Space

We detected urban green space cooling distance and direction using a semi-variance function [35], which is often used when there is a spatially-correlated distance or directional bias in the data. Our data are inherently spatially biased, which makes them appropriate for this function. The semi-variance function is defined as:

$$\gamma(h) = \frac{1}{2N(h)} \sum_{i=1}^{N(h)} [Z(x_i) - Z(x_i + h)]^2 \quad (6)$$

where, $\gamma(h)$ is the semi-variance, $Z(x)$ is the regional variable, $N(h)$ is of the sample size, and h is the separation distance. The spatial variation of the regional variable shows a stable value as the distance increases to a certain degree; that is, a partial sill. This distance is the maximum spatially-correlated interval, which, for this study, is the maximum cooling distance. The semi-variance function of the two-dimensional regional variable is also directional; when the ratio of two different directions is equal or close to 1, it shows isotropy, otherwise it will show anisotropy. The cooling distances of the different directions were derived from the semi-variance model parameters of ArcGIS10.3 geostatistical analyst toolkit.

Since the semi-variance function cannot be applied to aggregated urban green spaces (green space patches within a distance of less than 150 m from each other) with mutual cooling effects, we generated ten buffer rings of equidistant division from 0 m–300 m at 30 m intervals (corresponding to the resolution of the raster image) around the selected aggregated urban green spaces and calculated the average ground temperature of each interval. The point along the 0–300 m buffer distance at which the temperature semi-variance curve became stable, is approximately the cooling distance of that aggregate of urban green spaces.

2.3.4. Mitigating Effect of Green Space Spatial Distribution

To discover the relationship between the spatial distribution of urban green spaces and the heat island pattern, we used the k-nearest neighbor algorithm. This algorithm calculates a nearest neighbor index based on the mean distance from each feature to its nearest neighboring feature. Next, it identifies whether the distribution pattern of urban green spaces is aggregated or scattered. We calculated the k-nearest neighbor values using the Spatial Statistics Tools in ArcGIS10.3 and divided the nearest neighbor indices into different grades using the threshold value (Table 2). In addition, we calculated the percentage of area for each urban green space that is within each district to determine the influence of district on average temperature. We obtained urban green space aggregation degree and the area proportion of four districts in Baotou, including Kundulun, Qingshan, Donghe, and Jiuyuan, and the established the relationships between the aggregation degree, area proportion, and the mean temperature in each district.

Table 2. *k*-nearest neighbor index classification.

Nearest Neighbor Index	Type
0–0.5	Aggregated
0.5–1.0	More aggregated than random distribution
1.0	Random distribution
1.0–1.5	More scattered than random distribution
>1.5	Scattered

3. Results

3.1. Spatiotemporal Variations of UHI Intensity

From the temperature retrieval and heat island intensity classification (Equation (5) and Table 1), we found that the heat island intensities of Baotou were mostly classified as moderate, strong, or

very strong UHIs. These moderate to very strong UHIs were distributed in the downtown area, specifically in areas with relatively high building density or on unused land. In contrast, urban green spaces and their surrounding areas were classified as either no, or as weak heat islands. Extremely strong heat islands only accounted for a relatively small area, mainly located in the industrial area of Baotou (Figure 2).

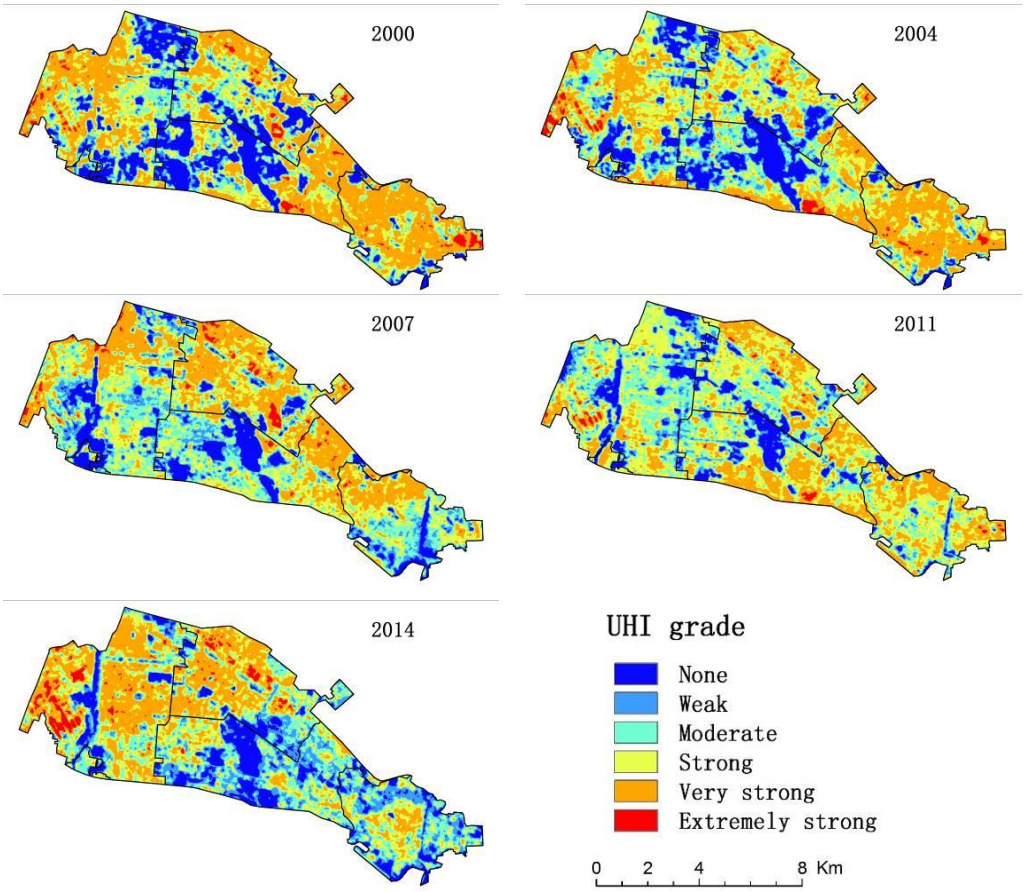

Figure 2. Intensity map of heat islands in Baotou. The UHI intensity was classified into six categories, with the colors from blue to red representing the intensity of UHIs from weak to strong.

Seven landscape indices were selected to measure UHI intensity, targeting four types of heat islands; moderate, strong, very strong, and extremely strong, reflecting their dynamic change within the five time periods (Figure 3). We found that the areas of moderate, strong, and very strong heat islands together accounted for a relatively large proportion of the total area (each accounting for about 25%). Areas of moderate and strong heat islands increased (from 13% and 21.7% to 20.9% and 35.7%, respectively, Figure 3a,b) before 2011, and then began to decrease (to 19.6% and 21.8%, respectively) by 2014. There was an initial increase in the number of moderate and strong heat island patches from 2000 to 2007, followed by a decrease in 2011, with the number of strong heat island patches increasing again in 2014. The areas of very strong and extremely strong heat islands first decreased (from 37.2% and 1.8% to 23.4% and 0.8%, respectively) and then increased (to 27.7% and 2.7%, respectively). However, the number of patches within the very strong and extremely strong heat island classifications showed little change over the study period. The total variation of heat island landscape shape indices were not obvious (Figure 3c), but the indices of moderate and strong heat islands were relatively high and diffuse in distribution, which is supported by the AI values (Figure 3e). However, overall, the pattern across all categories was considered to be aggregated in distribution, especially for the very strong heat island classification. There was a gradual decreasing trend (Figure 3d), ranging from 1.004 to 1.092, on

the mean patch fractal dimensions of the four heat island types, shown by the total FRAC_MN value for Baotou (Figure 3f). This indicates that these types of heat islands are relatively evenly-spaced in Baotou, and across all types, represented 84%–85% in the aggregation model (Figure 3g,h).

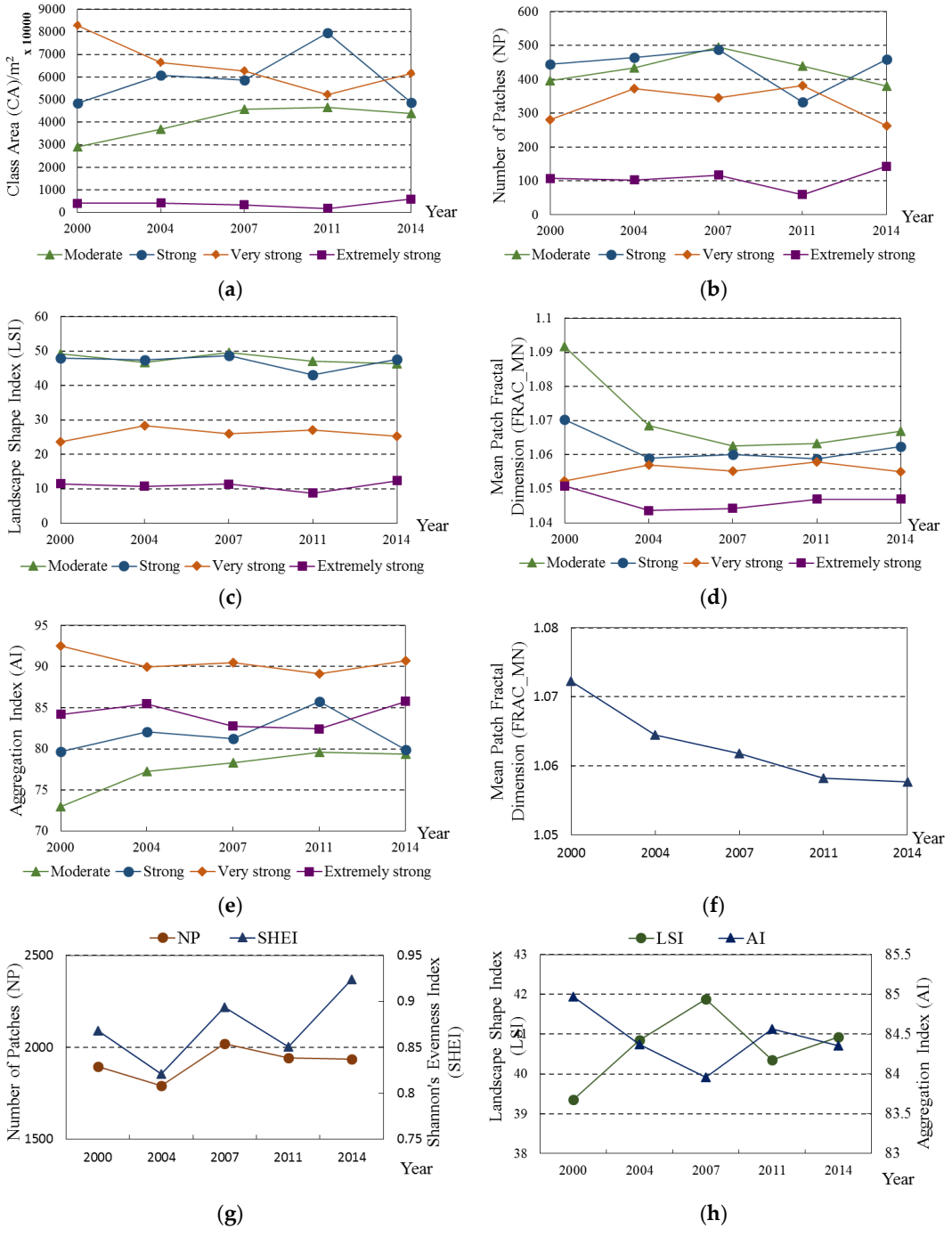

Figure 3. Chart of UHI intensity indices. (**a**) The total area, and (**b**) total number of each type of patch; (**c**) the landscape regular shape, and (**d**) the aggregation of each type, respectively. The higher the value of LSI, the larger the degree of more irregular shaped patches, but the greater value of AI indicates a higher degree of aggregation. (**e**) Represents the complexity of the patch border shape, with larger values indicating more complex shapes; (**f**–**h**) represent the dynamic change of total landscape structures for all five time periods, of which SHEI represents the non-uniformity of patch distribution. The SHEI with values of 1 indicates the uniform distribution of different patches.

3.2. Urban Green Spaces Cooling Effects

3.2.1. Urban Green Spaces Cooling Distance

Nine independently-distributed urban green spaces, whose surrounding temperatures had not been affected by adjacent green spaces, were selected for isotropic and anisotropic cooling distance analysis within the five periods of our remote sensing image data. There was a logarithmic relationship between both area and shape index with cooling distance (R^2 = 0.6 for both relationships) (Figure 4a,c), and a linear relationship between mean NDVI and cooling distance (a significance of 10%; Figure 4b). Urban green spaces with more area corresponded to a larger cooling distance; however, the influence distance tended to be stable with the increase of area. The shape of the urban green space patches also affected cooling distance, and cooling distance decreased with shape complexity. The internal cooling effect of high NDVI of urban green space was significant, and presented a positive correlation with cooling distance on the whole. However, this effect was not obvious because of the influence of other factors.

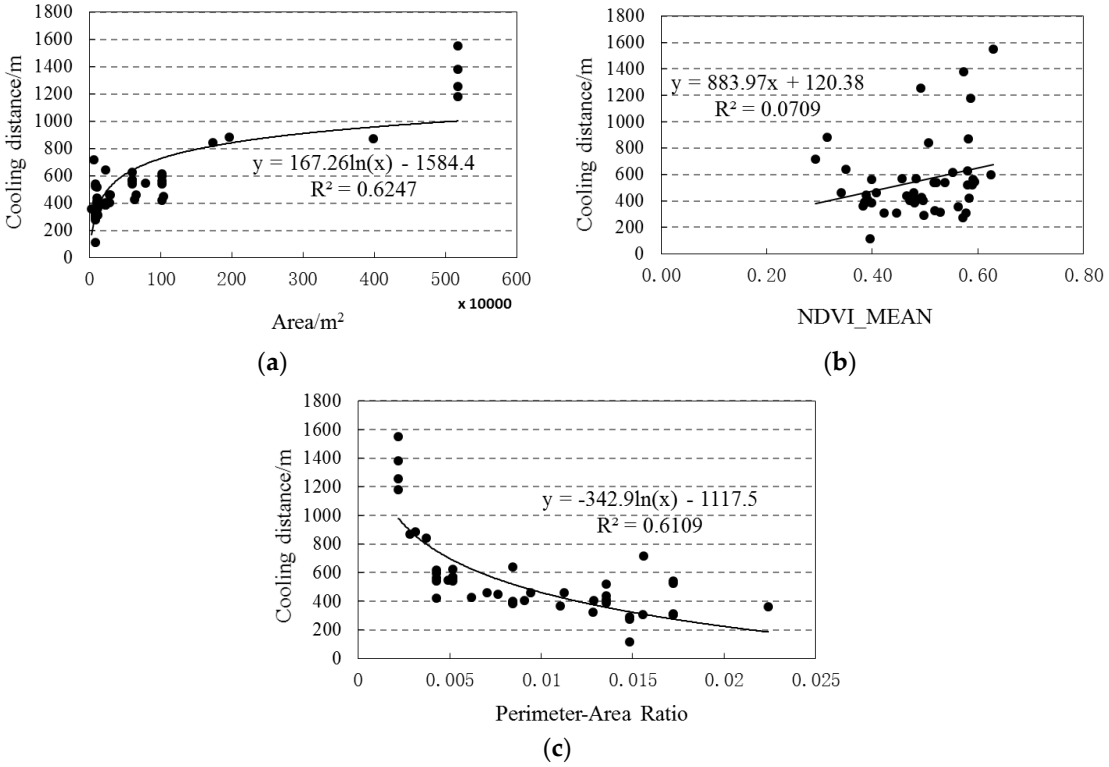

Figure 4. Relationships between urban green cooling distance, area, NDVI mean, and PARA. (**a**) represents the relationship between urban green space area and cooling distance in five time periods remote sensing image data; (**b**) represents the relationship between the mean NDVI of each urban green space and cooling distance in the same images; and (**c**) represents the relationship between shape index of each urban green space and the cooling distance in the same images.

Analysis of the urban green space aggregates identified that the surrounding temperature of the six selected sampling areas increased with distance and displayed a law of gradient variation (Figure 5). The variation tended to stable out around 180 m, before which the cooling magnitude was higher and after which the cooling magnitude was lower (<1 °C). Within 300 m, the cooling temperature was between 1.9 and 3.1 °C, and the maximum cooling distance was between 120 and 300 m.

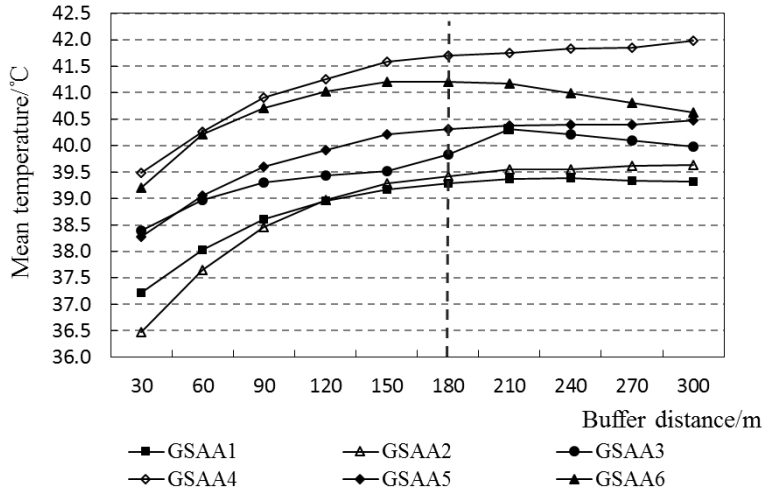

Figure 5. Cooling distance variation in surrounding area of selected urban green space aggregated areas (GSAA). Each polyline represents mean temperature within ten different buffer distances of selected urban green space aggregates in five time periods of remote sensing image data.

3.2.2. The Directivity of Urban Green Spaces Cooling Distance

The anisotropic cooling distance of the selected urban green space (Table 3) was associated with green space shape. The maximum cooling distance was on the semi-major axis of the green space, while the minimum distance was on the semi-minor axis. The cooling distance from the centroid of green space increased with green space area. However, there was no clear trend to follow for the cooling distance away from the green space border. The maximum directional cooling distance was between 150 and 454 m, while the minimum directional cooling distance was between 106 and 333 m.

Table 3. The selected urban green space cooling distance.

Urban Green Space	Area (m^2)	From the Green Space Border/m		From the Green Space Centroid/m	
		Maximum Cooling Distance	Minimum Cooling Distance	Maximum Cooling Distance	Minimum Cooling Distance
Qingshan Park	0.09×10^6	248	133	439	283
The People's Park	0.11×10^6	243	174	523	354
Jiuyuan Park	0.12×10^6	254	138	484	298
Bayi Park	0.23×10^6	269	185	499	405
Yiji Park	0.46×10^6	306	195	922	353
Labor Park	0.61×10^6	150	173	690	507
Arden Botanical Garden	1.02×10^6	276	106	999	432
Baogang Park	1.85×10^6	185	333	1015	754
Saihan Tara Ecological Park	4.94×10^6	454	218	2575	994

3.3. Cooling Effect of Urban Green Space Distribution

We found that urban green space distribution in Baotou was generally random or more scattered than random, and that green area accounted for 10%–40% of each district (Figure 6). Additionally, there was no significant correlation between the degree of aggregation of urban green spaces and mean temperature; however, the mean temperature did decrease as the urban green space distribution became dispersed. The ratio of urban green space area in each district presented a negative effect on mean temperature, and mean temperature tended to be lower with an increase of green space to area ratio. If the area ratio was greater than 50%, a more significant cooling effect could be identified.

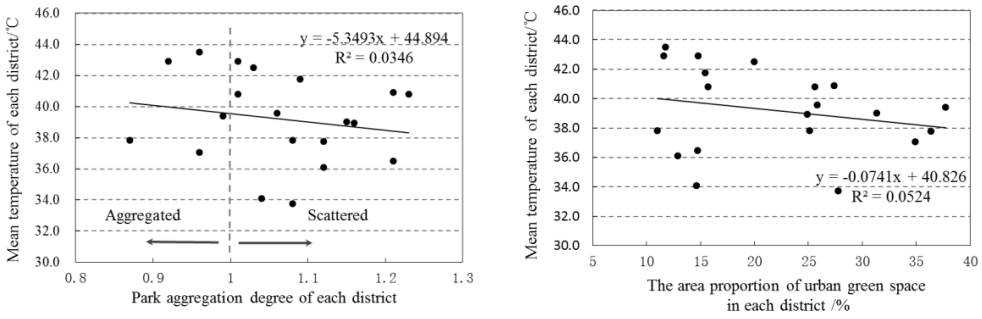

(**a**) (**b**)

Figure 6. Cooling effect diagram of urban green space distribution. (**a**) Represents the relationship between aggregation of urban green space of each district and mean temperature of each district in five time periods of remote sensing imagery data. When the value is 1, the urban green space distribution is random, when the value is less than 1, the distribution is aggregated, and when the value is more than 1 the distribution is scattered; and (**b**) represents the relationship between the proportion of area of urban green space in each district and mean temperature of each district in the same images.

4. Discussion

4.1. Relationship between the Urban Heat Island and Green Space

We found that areas with high building density have more UHI, in contrast to urban green spaces and their surrounding areas where no, or only weak, heat islands were found. The amount of area of urban green space was a strong predictor for mitigating UHI effects, suggesting that larger green spaces have larger cooling distances [13,32,36]. However, a strong positive logarithmic relationship between area and the cooling distance (R^2 = 0.62) was also found, which suggested that with the increase of urban green space area the cooling effect plateaus. Mean NDVI had a weak linear correlation with cooling distance (R^2 = 0.07). Diverse land cover across the urban green space was likely the main cause for this, *i.e.*, species composition [17], community structure [18], internal water bodies, and permeable surface [19,20] all likely contribute to the cooling effect. Accumulative or area weighted index, such as NDVI or percent cover of woody vegetation [27], might be a good candidate for analysis of green space mitigating effects of the urban heat island effects in further studies. We also found that the spatial configuration of green space had a significant effect on UHI. This result is consistent with findings from previous studies [36], in which it was reported that the more regularly spaced the urban green spaces are, the lower the surface temperatures. However, Zhou *et al.* (2011) suggested that LST decreased through the increase in the amount of green space edge, which enhances the thermal exchange between the green space and its surrounding areas [27]. We suggest the relatively small size of green spaces in this study was insufficient to identify significant cooling effects [37].

The directivity of urban green spaces cooling distance is anisotropic, and does have an effect on LST pattern. The maximum cooling distances (150 to 454 m) and minimum cooling distances (106 to 333 m), respectively, corresponded to the directions of the radius of the urban green spaces. The cooling effects of urban green spaces were related to their shape; green spaces in simple shapes showed isotropy while those with complex shapes showed the contrary. Interestingly, the different directions did not have the same cooling distances. However, the semi-variance function was only suitable for analyzing individual green spaces rather than concentrated spaces, which could influence the result. Due to the limited capacity of the function itself, and because the surface temperature of the surrounding areas was affected by the similarity of aggregated green spaces with their surrounding area, the cooling distance was enlarged. For this reason, we used the buffer zone method to calculate the cooling effect of different urban green spaces in concentrated areas. We found that the variation of temperature was higher before 180 m, after which the variation of temperature was lower (<1°C), and the cooling temperature was between 1.9 and 3.1 °C.

The ground surface temperature, and its aggregation degree, showed a positive correlation with the ground surface temperature (Figure 6a). This meant that the temperature was lowered when green spaces were scattered. This result was contrary to the conclusion drawn by Wang *et al.* (2014), that there was a negative correlation between aggregation degree and urban ground surface temperature [38]. On one hand, it is related to the size of green spaces and the mean distance (or arrangement) between each of them. In Li *et al.* (2012), a similar result to Wang *et al.* (2014) was observed in Beijing, a city which is dominated by small patches [32]. Located near paved roads, small green spaces that are scattered across a city usually have a high thermal load and are unlikely to produce significant cool island effects [39], with the mean distance of those green spaces larger than its cooling effects. As a result, the cooling effect of aggregated urban green spaces is limited. However, in our study, the mean distance between each green space and average green space size is 151.2 m and 2.1×10^5 m^2 respectively, providing more area and greater distances of urban green spaces to analyze. On the other hand, the relationship between mean temperature and the green spaces area ratio of each district showed negative correlation (Figure 6b). When the ratio was greater than 50%, the influence might become clearer. Thus, during the planning of urban green spaces, we should consider their spatial distribution and evenly distribute them as much as possible. We feel that a rational design of urban green space area would not only mitigate the UHI effect, but also play a role of leisure and recreation, earthquake preparedness, and disaster reduction, *etc.*

4.2. Implications for Urban Planning

Vegetation management, such as planting more trees, should be considered an effective approach to cooling the heated city [27]. This has already been done for Beijing, where they planned the wedge green belt to increase tree canopy cover to cool down the metropolitan area [40]. The size of an urban green space is an important factor that effect UHI dynamics that is widely accepted. However, it is infeasible to account for the building expense that green spaces come with in some urban area. We found that not only spatial configuration but also distribution of green space affected LST, which also supported by other researches [27,32,36]. When public space is limited, different spatial arrangements of land cover features can significantly decrease LST [27], e.g., encouraging private "greening" areas rather than building new expensive small-medium sized parks [39]; increasing patch density of the green space, rather than expanding the green space cover [36]; and covering roofs or facades with plants mitigating urban thermal environment [39,41], are all feasible options.

5. Conclusions

We analyzed five time periods of remote sensing image data to extract surface temperature and urban green spaces of built-up areas in Baotou using the mono-window algorithm. We also analyzed five time periods of UHI intensity change in Baotou with the landscape index, based on the effect of urban green spaces on UHI pattern using the methods of semi-variance function, buffer zone method, and aggregation degree. The conclusions as follow:

(1) The cooling distance of an urban green space varied with its size and shape, and the cooling distance showed anisotropy. Within a certain threshold, the greater urban green space area and mean NDVI clearly corresponded to a larger cooling distance. With increasing of shape complexity of the green space, the cooling distance declined in certain green space areas. According to the semi-variance function, the cooling distance was directional, the maximum cooling distance was on the semi-major axis of the green space, and the cooling distance was between 150 and 454 m, while the minimum distance was on the semi-minor axis and the cooling distance was between 106 and 333 m.

(2) The distribution of urban green space plays a key role in mitigating the UHI effect. Within a certain space, in terms of the cooling effect, evenly-distributed green spaces have greater effects than aggregated distributed green spaces. Therefore, within the limited urban space, relatively scattered and evenly-distributed green spaces are a potential solution for urban planning to mitigate the UHI effect.

Acknowledgments: This work is supported by the Project of Higher Educational Scientific Research Projects of Inner Mongolia (Grant No. NJZY14249) and the Natural Science Foundation of Inner Mongolia (Grant No. 2014MS0401).

Author Contributions: Tongliga Bao proposed and developed the research design, data processing, manuscript writing and results interpretation. Xueming Li supervised all the manuscript work and revised the manuscript extensively. Jing Zhang contributed to the introduction part, data processing, charts and tables design, discussion writing and manuscript revision. Yingjia Zhang and Shenzhen Tian coordinated the data acquisition, paper censor and corrected and modified the manuscript.

Conflicts of Interest: The authors declare no conflict of interest.

References

1. UN. *World Urbanization Prospects: The 2011 Revision Highlights*; United Nations: New York, NY, USA, 2012.
2. Mackey, C.W.; Lee, X.; Smith, R.B. Remotely sensing the cooling effects of city scale efforts to reduce urban heat island. *Build. Environ.* **2012**, *49*, 348–358. [CrossRef]
3. Zhou, D.; Zhao, S.; Liu, S.; Zhang, L.; Zhu, C. Surface urban heat island in China's 32 major cities: Spatial patterns and drivers. *Remote Sens. Environ.* **2014**, *152*, 51–61. [CrossRef]
4. Oke, T.R. The energetic basis of the urban heat island. *Q. J. Roy. Meteor. Soc.* **1982**, *108*, 1–24. [CrossRef]
5. Smargiassi, A.; Goldberg, M.S.; Plante, C.; Fournier, M.; Baudouin, Y.; Kosatsky, T. Variation of daily warm season mortality as a function of micro-urban heat islands. *J. Epidemiol. Community Health* **2009**, *63*, 659–664. [CrossRef] [PubMed]
6. Debbage, N.; Shepherd, J.M. The urban heat island effect and city contiguity. *Comput. Environ. Urban Syst.* **2015**, *54*, 181–194. [CrossRef]
7. Stone, B.; Vargo, J.; Liu, P.; Habeeb, D.; DeLucia, A.; Trail, M.; Hu, Y.; Russell, A. Avoided heat-related mortality through climate adaptation strategies in three US cities. *PLOS ONE* **2014**, *9*, e100852.
8. Liu, K.; Su, H.; Zhang, L.; Yang, H.; Zhang, R.; Li, X. Analysis of the urban heat island effect in Shijiazhuang, China using satellite and airborne data. *Remote Sens.* **2015**, *7*, 4804–4833. [CrossRef]
9. Weaver, C.P.; Cooter, E.; Gilliam, R.; Gilliland, A.; Grambsch, A.; Grano, D.; Hemming, B.; Hunt, S.W.; Nolte, C.; Winner, D.A.; *et al*. A preliminary synthesis of modeled climate change impacts on us regional ozone concentrations. *Bull. Am. Meteorol. Soc.* **2009**, *90*, 1843–1863.
10. Georgi, N.J.; Zafiriadis, K. The impact of park trees on microclimate in urban areas. *Urban Ecosyst.* **2006**, *9*, 195–209. [CrossRef]
11. Feyisa, G.L.; Dons, K.; Meilby, H. Efficiency of parks in mitigating urban heat island effect: An example from Addis Ababa. *Landsc. Urban. Plan* **2014**, *123*, 87–95. [CrossRef]
12. Zhang, Y.; Chen, L.; Wang, Y.; Chen, L.; Yao, F.; Wu, P.; Wang, B.; Li, Y.; Zhou, T.; Zhang, T. Research on the contribution of urban land surface moisture to the alleviation effect of urban land surface heat based on Landsat 8 data. *Remote Sens.* **2015**, *7*, 10737–10762. [CrossRef]
13. Oliveira, S.; Andrade, H.; Vaz, T. The cooling effect of green spaces as a contribution to the mitigation of urban heat: A case study in Lisbon. *Build. Environ.* **2011**, *46*, 2186–2194. [CrossRef]
14. Susca, T.; Gaffin, S.R.; Dell'Osso, G.R. Positive effects of vegetation: Urban heat island and green roofs. *Environ. Pollut.* **2011**, *159*, 2119–2126. [CrossRef] [PubMed]
15. Zhao, Q.; Myint, S.W.; Wentz, E.A.; Fan, C. Rooftop surface temperature analysis in an urban residential environment. *Remote Sens.* **2015**, *7*, 12135–12159. [CrossRef]
16. Bowler, D.E.; Buyung-Ali, L.; Knight, T.M.; Pullin, A.S. Urban greening to cool towns and cities: A systematic review of the empirical evidence. *Landsc. Urban. Plan.* **2010**, *97*, 147–155. [CrossRef]
17. Oke, T.R. *Boundary Layer Climates*; Methuen& Co., Ltd.: London, UK; Methuen, Inc.: New York, NY, USA, 1988.
18. Onishi, A.; Cao, X.; Ito, T.; Shi, F.; Imuraa, H. Evaluating the potential for urban heat-island mitigation by greening parking lots. *Urban For. Urban Green.* **2010**, *9*, 323–332. [CrossRef]
19. Owen, T.W.; Carlson, T.N.; Gillies, R.R. An assessment of satellite remotely-sensed land cover parameters in quantitatively describing the climatic effect of urbanization. *Int. J. Remote. Sens.* **1998**, *19*, 1663–1681. [CrossRef]
20. Buyantuyev, A.; Wu, J. Urban heat islands and landscape heterogeneity: Linking spatiotemporal variations in surface temperatures to land-cover and socioeconomic patterns. *Landsc. Ecol.* **2010**, *25*, 17–33. [CrossRef]

21. Chun, B.; Guldmann, J.M. Spatial statistical analysis and simulation of the urban heat island in high-density central cities. *Landsc. Urban. Plan.* **2014**, *1225*, 76–88. [CrossRef]
22. Jenerette, D.; Jarlan, S.; Brazel, A.; Jones, N.; Larsen, L.; Stefanov, W. Regional relationships between surface temperature, vegetation, and human settlement in a rapidly urbanizing ecosystem. *Landsc. Ecol.* **2007**, *22*, 353–365. [CrossRef]
23. Ren, Z.; He, X.; Zheng, H.; Zhang, D.; Yu, X.; Shen, G.; Guo, R. Estimation of the relationship between urban park characteristics and park cool island intensity by remote sensing data and field measurement. *Forests* **2013**, *4*, 868–886. [CrossRef]
24. Li, J.; Song, C.; Cao, L.; Zhu, F.; Meng, X.; Wu, J. Impacts of landscape structure on surface urban heat islands: A case study of Shanghai, China. *Remote Sens. Environ.* **2011**, *115*, 3249–3263. [CrossRef]
25. Chen, X.; Zhao, H.; Li, P.; Yin, Z. Remote sensing image-based analysis of the relationship between urban heat island and land use/cover changes. *Remote Sens. Environ.* **2006**, *104*, 133–146. [CrossRef]
26. Connors, J.P.; Galletti, C.S.; Chow, W.T.L. Landscape configuration and urban heat island effects: Assessing the relationship between landscape characteristics and land surface temperature in Phoenix, Arizona. *Landsc. Ecol.* **2013**, *28*, 271–283. [CrossRef]
27. Zhou, W.; Huang, G.; Cadenasso, M.L. Does spatial configuration matter? Understanding the effects of land cover pattern on land surface temperature in urban landscapes. *Landsc. Urban Plan.* **2011**, *102*, 54–63.
28. Hamada, S.; Tanaka, T.; Ohta, T. Impacts of land use and topography on the cooling effect of green areas on surrounding urban areas. *Urban For. Urban Green.* **2013**, *12*, 426–434. [CrossRef]
29. Doick, K.J.; AndrewPeace; Hutchings, T.R. The role of one large green space in mitigating London's nocturnal urban heat island. *Sci. Total Environ.* **2014**, *493*, 662–671. [CrossRef] [PubMed]
30. Hamada, S.; Ohta, T. Seasonal variations in the cooling effect of urban green area on surrounding urban areas. *Urban For. Urban Green.* **2010**, *9*, 15–24. [CrossRef]
31. Alcoforado, M.J.; Andrade, H.; Lopes, A.; Vasconcelos, J. Application of climatic guidelines to urban planning: The example of Lisbon (Portugal). *Landsc. Urban. Plan.* **2009**, *90*, 56–65. [CrossRef]
32. Li, X.; Zhou, W.; Ouyang, Z.; Xu, W.; Zheng, H. Spatial pattern of greenspace affects land surface temperature: Evidence from the heavily urbanized Beijing metropolitan area, China. *Landsc. Ecol.* **2012**, *27*, 887–898. [CrossRef]
33. Wu, H.; Ye, L.; Shi, W.; Clarke, K.C. Assessing the effects of land use spatial structure on urban heat islands using HJ-1B remote sensing imagery in Wuhan, China. *Int. J. Appl. Earth Obs. Geoinform.* **2014**, *32*, 67–78. [CrossRef]
34. Du, P.; Tan, K.; Xia, J.; Zhao, Y. *Method and Practice of Urban Environmental Remote Sensing*; Science Press: Beijing, China, 2014. (In Chinese)
35. Oliver, M.A. Kriging: A method of interpolation for geographical information systems. *Int. J. Geogr. Inf. Syst.* **1990**, *4*, 313–332. [CrossRef]
36. Maimaitiyiming, M.; Ghulam, A.; Tiyip, T.; Pla, F.; Latorre-Carmona, P.; Halik, Ü.; Sawut, M.; Caetano, M. Effects of green space spatial pattern on land surface temperature: Implications for sustainable urban planning and climate change adaptation. *ISPRS J. Photogramm.* **2014**, *89*, 59–66. [CrossRef]
37. Zhang, X.; Zhong, T.; Feng, X.; Wang, K. Estimation of the relationship between vegetation patches and urban land surface temperature with remote sensing. *Int. J. Remote Sens.* **2009**, *30*, 2105–2118. [CrossRef]
38. Wang, W.; Deng, R. Alleviative effects of urban green space on urban heat island. *Geospatial Inf.* **2014**, *12*, 52–54. (In Chinese).
39. Rotem-Mindali, O.; Michael, Y.; Helman, D.; Lensky, I.M. The role of local land-use on the urban heat island effect of Tel Aviv as assessed from satellite remote sensing. *Appl. Geogr.* **2015**, *56*, 145–153. [CrossRef]
40. Tong, H.; Liu, H.; Li, Y.; Sang, J.; Hu, F. Acyuality of summer urban heat island and the impact of urban planning "wedge-shaped" greenland to reducing the intensity of urban heat island in Beijing. *J. Appl. Meteorol. Sci.* **2005**, *16*, 257–266. (In Chinese).
41. Wong, J.K.W.; Lau, S.K. From the "urban heat island" to the "green island"? A preliminary investigation into the potential of retrofitting green roofs in Mongkok district of Hongkong. *Habitat Int.* **2013**, *39*, 25–35.